The lipid structure of the glycosylphosphatidylinositol-anchored mucin-like sialic acid acceptors of Trypanosoma cruzi changes during parasite differentiation from epimastigotes to infective metacyclic trypomastigote forms

THE JOURNAL OF BIOLOGICAL CHEMISTRY
Vol. 270, No. 45, Issue of November 10, pp. 27244–27253, 1995
Printed in U.S.A.

The Lipid Structure of the Glycosylphosphatidylinositol-anchored Mucin-like Sialic Acid Acceptors of *Trypanosoma cruzi* Changes during Parasite Differentiation from Epimastigotes to Infective Metacyclic Trypomastigote Forms*

(Received for publication, June 19, 1995, and in revised form, August 28, 1995)

Alvaro Acosta Serrano‡§, Sergio Schenkman‡, Nobuko Yoshida‡, Angela Mehlert¶, Julia M. Richardson¶‖, and Michael A. J. Ferguson¶**

From the ‡Departmento de Microbiologia, Immunologia e Parasitologia, Escola Paulista de Medicina, Universidade Federal de São Paulo, Rua Botucatu, 862, 8° andar, 04023-062, São Paulo, S.P., Brazil and the ¶Department of Biochemistry, University of Dundee, Dundee DD1 4HN, Scotland, United Kingdom

The major acceptors of sialic acid on the surface of metacyclic trypomastigotes, which are the infective forms of *Trypanosoma cruzi* found in the insect vector, are mucin-like glycoproteins linked to the parasite membrane via glycosylphosphatidylinositol anchors. Here we have compared the lipid and the carbohydrate structure of the glycosylphosphatidylinositol anchors and the *O*-linked oligosaccharides of the mucins isolated from metacyclic trypomastigotes and noninfective epimastigote forms obtained in culture. The single difference found was in the lipid structure. While the phosphatidylinositol moiety of the epimastigote mucins contains mainly 1-*O*-hexadecyl-2-*O*-hexadecanoylphosphatidylinositol, the phosphatidylinositol moiety of the metacyclic trypomastigote mucins contains mostly (~70%) inositol phosphoceramides, consisting of a $C_{18:0}$ sphinganine long chain base and mainly $C_{24:0}$ and $C_{16:0}$ fatty acids. The remaining 30% of the metacyclic phosphatidylinositol moieties are the same alkylacylphosphatidylinositol species found in epimastigotes. In contrast, the glycosylphosphatidylinositol glycan cores of both molecules are very similar, mainly Manα1–2Manα1–2Manα1–6Manα1–4GlcN. The glycans are substituted at the GlcN residue and at the third αMan distal to the GlcN residue by ethanolamine phosphate or 2-aminoethylphosphonate groups. The structures of the desialylated *O*-linked oligosaccharides of the metacyclic trypomastigote mucin-like molecules, released by β-elimination with concomitant reduction, are identical to the structures reported for the epimastigote mucins (Previato, J. O., Jones, C., Gonçalves, L. P. B., Wait, R., Travassos, L. R., and Mendoça-Previato, L. (1994) *Biochem. J.* 301, 151–159). In addition, a significant amount of nonsubstituted *N*-acetylglucosaminitol was released from the mucins of both forms of the parasite. Taken together, these results indicate that when epimastigotes transform into infective metacyclic trypomastigotes, the phosphatidylinositol moiety of the glycosylphosphatidylinositol anchor of the major acceptor of sialic acid is modified, while the glycosylphosphatidylinositol anchor and *O*-linked sugar chains remain essentially unchanged.

Trypanosoma cruzi, the protozoan parasite that causes Chagas' disease in humans, has a complex life cycle alternating between the insect vector and the mammalian host. In the vector, it multiplies as noninfective epimastigotes that migrate to the hindgut and differentiate into infective metacyclic trypomastigotes. During the insect blood meal, the metacyclic trypomastigotes are deposited with the feces and urine near a skin wound, initiating the natural infection.

T. cruzi is unable to synthesize sialic acids (SA),[1] but it expresses a unique *trans*-sialidase (TS), which transfers α2–3-linked SA from host glycoproteins and glycolipids to acceptors containing terminal β-galactosyl residues present on the parasite surface (reviewed in Refs. 1–4). Several studies characterizing the nature and structure of the SA acceptors have been published. These acceptors are abundant on the parasite surface and were first described as major surface glycoproteins of epimastigotes by Alves and Colli (5), who called them bands A, B, and C. Subsequently, a similar cell surface glycoprotein complex, called GP24, GP31, and GP37 was described by Ferguson *et al.* (6), and Previato *et al.* (7) first described a 43-kDa SA acceptor. More recently, they have been called 38/43 glycoconjugates (8), and the so called epimastigote lipophosphoglycan-like molecule could belong to the same family of molecules (9). In metacyclic trypomastigote forms, the SA acceptors were reported originally as the 35/50-kDa antigens (10, 11) that were subsequently defined as mucin-like glycoproteins (12). In the trypomastigote forms found in mammals, the SA acceptors were described as a group of molecules that share the stage-specific epitope 3 (Ssp-3) (13), an epitope dependent on parasite

* This work was supported by grants from the Fundação de Amparo à Pesquisa do Estado de São Paulo, Conselho Nacional de Desenvolvimento Científico e Tecnológico, Brazil, the UNDP/World Bank/WHO Special Program for Research and Training in Tropical Diseases, The Rockefeller Foundation, National Institutes of Health Grant RTW00227-03, and the Wellcome Trust. The costs of publication of this article were defrayed in part by the payment of page charges. This article must therefore be hereby marked "*advertisement*" in accordance with 18 U.S.C. Section 1734 solely to indicate this fact.

§ Supported by a graduate fellow from CONICIT (Venezuela) and by a WHO Fellowship Training Grant in Tropical Diseases. To whom correspondence should be addressed: Disciplina de Biologia Celular, Escola Paulista de Medicina, R. Botucatu 862/8A, 04023-062 São Paulo, S.P., Brazil. Fax: 55-11-549-2127; E-mail: alvaro.dmip@epm.br.

‖ Present address: School of Chemistry, St. Andrew University, St. Andrew KY16 9ST, Scotland, United Kingdom.

** Howard Hughes International Research Scholar.

[1] The abbreviations used are: SA, sialic acid(s); TS, *trans*-sialidase; GPI, glycosylphosphatidylinositol; PI, phosphatidylinositol; ES-MS, electrospray-mass spectrometry; GC-MS gas chromatography-mass spectrometry; HPTLC, high-performance thin layer chromatography; HPLC, high-performance liquid chromatography; AHM*, [1-^{3}H]2,5-anhydromannitol; GlcNAc-ol, *N*-acetylglucosaminitol; HexNAc-ol, *N*-acetylhexosaminitol; LPPG, lipopeptidophosphoglycan; Gu, glucose units; 2-AEP, 2-aminoethylphosphonate; PAGE, polyacrylamide gel electrophoresis.

sialylation (14), and were also identified as mucin-like molecules that appear larger than the epimastigote and metacyclic mucins on SDS-polyacrylamide gel electrophoresis (15, 16). These trypomastigote mucins also contain some terminal α-galactosyl residues (16). In summary, these mucin-like molecules are glycoproteins rich in threonine and serine that are linked to the parasite membrane via a glycosylphosphatidylinositol (GPI) anchor and that contain novel *O*-linked oligosaccharides. The *O*-linked oligosaccharides are attached to the protein via GlcNAc residues and act as SA acceptor sites for the parasite TS. The chemical structure of *O*-linked oligosaccharides of epimastigote mucins of G (8) and Y (17) strains have recently been elucidated. They are quite similar but differ in their average size and in some of the Gal linkages. The glycan structure of the GPI anchor of the epimastigote mucin (Y strain) has also been reported (17).

Several lines of evidence suggest that the 35/50-kDa mucins of metacyclic-trypomastigotes are involved in host cell invasion. Monoclonal antibodies directed against the mucin, and the purified molecule itself, are able to inhibit parasite entry (10, 18), and the 35/50-kDa antigens are capped and locally released during invasion (12). Epimastigotes are unable to enter mammalian cells but express large amounts of mucins with similar size recognized by the same monoclonal antibodies. Therefore, we decided to investigate possible subtle structural differences between the mucins of these two stages. We found that, after differentiation of epimastigotes into metacyclic forms, the lipid portion is modified, while the oligosaccharide chains and the glycan structure of the GPI are conserved. This lipid change might correlate with the increased infectivity of metacyclic forms and the ability of the parasite to shed the mucins upon invasion of the host cell (12).

MATERIALS AND METHODS

Parasites—Epimastigotes of *T. cruzi* strain G (19) were grown at 28 °C in liver-infusion tryptose medium (20) containing 10% fetal bovine serum. Metacyclic trypomastigotes were purified from cultures at stationary phase by passage through a diethylaminoethyl cellulose column, as described in Ref. 19. The purity of the metacyclic trypomastigote preparations were estimated by morphology and/or by complement-mediated lysis assay using normal human sera.

Purification of Mucins—Mucins from epimastigotes and metacyclic trypomastigotes were extracted as described for the lipophosphoglycan of *Leishmania donovani* (21). Briefly, parasites (~7×10^{10} epimastigotes and ~8×10^{10} metacyclic trypomastigotes) were freeze-dried and placed in a sonicating water bath for 10 min with 50 ml of chloroform/methanol/water (1:2:0.8, by volume). After centrifugation (2,000 × *g*, 5 min) the insoluble material was re-extracted twice more, as described above, and the final insoluble pellet was used as a source of delipidated parasites. The pooled chloroform/methanol/water soluble fractions were evaporated under nitrogen, and the residue was extracted with 50 ml of butan-1-ol/water (2:1, by volume). The butan-1-ol phase, containing the lipid fraction (F1) was collected, and the aqueous phase (F2) was washed twice with 25 ml of water-saturated butan-1-ol and concentrated. The delipidated parasites were extracted by sonication (three times) with 25 ml of 9% butanol in water. The soluble material was pooled, concentrated, and freeze-dried to produce a polar fraction (F3). Most of the mucins from epimastigotes were recovered in F2, while mucins of metacyclic trypomastigotes were recovered in the F3 fraction. The mucins were resuspended in 0.5 ml of 0.1 M ammonium acetate in 5% propan-1-ol (v/v) (buffer A) and fractionated on an octyl-Sepharose column (10 × 0.5 cm), previously equilibrated in buffer A. The column was washed with 15 ml of buffer A and eluted with a linear gradient over 100 ml at a flow rate of 12 ml/h, starting with buffer A and ending with 60% (v/v) propan-1-ol in water. Fractions of 1 ml were assayed for reactivity with the monoclonal antibody 10D8 (10) by using a chemiluminescent dot-blotting assay (16). The immunoreactive material from the column was pooled, dried by rotatory evaporation, resuspended in water, and freeze-dried to remove traces of ammonium acetate. For the material submitted to lipid analysis, the samples were further partitioned between water and butan-1-ol to remove any remaining phospholipid and/or glycolipid contaminants. The aqueous phase was washed twice more with water-saturated butanol and freeze-dried again.

Nitrous Acid Deamination and NaB^3H_4 Reduction of GPI Neutral Glycans and Recovery of the Phosphatidylinositol Moieties—About 20 nmol of 35/50-kDa mucin of epimastigotes and metacyclic trypomastigotes, as judged by the *myo*-inositol content (see below) were freeze-dried, resuspended in 50 μl of 0.3 M sodium acetate, pH 4.0, and washed three times with 100 μl of butan-1-ol saturated with water. Then 25 μl of 1 M sodium nitrite was added to the aqueous phase (two times at 1-h intervals), and deamination was performed for 2 h at 37 °C. The released phosphatidylinositol (PI) moieties were recovered by three extractions with 100 μl of butan-1-ol saturated with water and analyzed by electrospray-mass spectrometry (ES-MS), as described below. The deaminated molecules remaining in the aqueous phase were reduced with NaB^3H_4, as described in Ref. 22, and repurified by chromatography on a Sephadex G-10 column, where they eluted in the void volume. The deaminated and NaB^3H_4-reduced mucins were then dephosphorylated in 48% aqueous HF for 60 h at 0 °C and re-*N*-acetylated, and the GPI neutral glycans were purified from radiochemical contaminants by downward paper chromatography and high voltage paper electrophoresis (22). The ^{3}H-labeled neutral glycans were analyzed by Bio-Gel P4 chromatography and Dionex high-performance anion-exchange chromatography. The elution positions of the radiolabeled glycans were expressed in glucose units (Gu) and Dionex units, respectively, by linear interpolation of the elution position between adjacent glucose oligomer internal standards (22).

Microsequencing of the GPI Glycan Cores—Three aliquots (20,000 cpm) of the neutral glycan fractions recovered from the Bio-Gel P4 column were dried in speed-vac and subjected to digestion with jack bean α-mannosidase (Boehringer Mannheim), *Aspergillus saitoi* Manα1–2Man-specific α-mannosidase (Oxford Glycosystems) and by partial acetolysis. Digestions were carried out with 0.75 units of jack bean α-mannosidase in 30 μl of 0.1 M sodium acetate buffer, pH 5.0, for 16 h at 37 °C or with 0.01 units of *A. saitoi* α-mannosidase in 10 μl of 0.1 M sodium acetate buffer, pH 5.0, for 16 h at 37 °C. Acetolysis was performed as described in Ref. 23. The products were analyzed by high performance thin layer chromatography (HPTLC) on silica gel 60 plates (Merck) using solvent A, propan-1-ol/acetone/water (9:6:4, by volume). Radioactive glycans were detected with a radioactivity linear analyzer (Raytest RITA) and visualized by fluorography after spraying with En^{3}Hance (DuPont NEN). A set of standards, terminating in [1-^{3}H]2,5-anhydromannitol (AHM*), was prepared by partial acid hydrolysis (23) of authentic Manα1–2Manα1–2Manα1–6Manα1–4AHM*, prepared from *T. cruzi* lipopeptidophosphoglycan (LPPG) (24). This so called Man4 ladder contains a mixture of Manα1–2Manα1–2Manα1–6Manα1–4AHM* (M4), Manα1–2Manα1–6Manα1–4AHM* (M3), Manα1–6Manα1–4AHM* (M2), Manα1–4AHM* (M1), and AHM*.

Location of the Ethanolamine Phosphate and 2-Aminoethylphosphonate Groups—This method was adapted from Ref. 23. Deaminated and NaB^3H_4-reduced mucins, 500,000 cpm (before dephosphorylation with aqueous HF), were subjected to partial acid hydrolysis in 500 μl of 0.1 M trifluoroacetic acid (100 °C, 12 h). The samples were dried in a speed-vac and redried twice from 200 μl of water. The hydrolysates were then split into three portions and treated as follows: (i) dephosphorylated with aqueous HF (60 h, 0 °C), (ii) treated with jack bean α-mannosidase prior to dephosphorylation with aqueous HF, or (iii) passed directly through a 0.2-ml QAE-Sephadex A-25 column. The products were analyzed by HPTLC using solvent A, as described above.

Mild Alkaline Treatment of 35/50-kDa Mucins and Fractionation of Oligosaccharitols—About 200 nmol of metacyclic 35/50-kDa mucin was freeze-dried twice, resuspended in 250 μl of 0.1 M NaOH containing 250 mM NaB^2H_4, and incubated for 24 h at 37 °C. The sample was acidified with 1 M acetic acid, desalted by passage through 0.6 ml of AG 50-X12 (H^+) (Bio-Rad), and dried, and boric acid was removed by co-evaporation with 250 μl of 5% acetic acid in methanol (three times) and with 250 μl of methanol (three times). Residual acetic acid was removed by co-evaporation with 50 μl of toluene (two times). Radiolabeled oligosaccharitols were prepared from freeze-dried mucins resuspended in 15 μl of 0.1 M of NaOH containing 36 mM NaB^3H_4 (13.6 Ci/mmol, DuPont NEN) and incubated for 24 h at 37 °C, followed by desalting as described above. Released radiolabeled oligosaccharitols were purified from radiochemical contaminants by descending paper chromatography on Whatman 3MM paper in butan-1-ol/ethanol/water (4:1:0.6, by volume) and digested with 50 mM *Arthrobacter ureafaciens* sialidase (Oxford Glycosystems) in 25 μl of 50 mM sodium acetate (pH 5.0) for 20 h at 37 °C. After desalting (as described below for the exoglycosidase digests) the neutral oligosaccharitols were fractionated by HPLC using a 5-μm hydrophilic interaction Glycoplex™ column (200 × 46 mm,

PolyLC Inc.). Briefly, samples were dissolved in 80% acetonitrile, water, and the column was eluted with an 80-ml gradient from 80 to 60% acetonitrile in water, at 1 ml/min. In preparative experiments, some of the radiolabeled material was added to the NaB^2H_4-reduced material to act as a tracer.

Purified oligosaccharitols obtained by fractionation on the Glycoplex™ HPLC column were submitted to exoglycosidase digestion, as described below, or to mild acid hydrolysis (200 μl of 40 mM trifluoroacetic acid for 1 h at 100 °C) to preferentially cleave Gal*f* glycosidic bonds (25), dried in a speed-vac, redried twice from 200 μl of water and re-*N*-acetylated as described in Ref. 22. The products were analyzed by Bio-Gel P4 chromatography.

Exoglycosidase Digestion—Neutral ^{3}H-labeled oligosaccharitols were analyzed before and after exoglycosidase digestion by HPTLC using solvent B, butan-1-ol/acetone/water (6:5:4, by volume). Oligosaccharitols were digested with 0.75 units of coffee bean α-galactosidase (Boehringer Mannheim) in 30 μl of 0.1 M sodium citrate/phosphate buffer, pH 6.0, for 16 h at 37 °C, with 2.5 units of fresh bovine testicular β-galactosidase (Boehringer Mannheim) in 20 μl of 0.1 M sodium citrate/phosphate buffer, pH 4.5, for 16 h at 37 °C, or with 0.1 units of jack bean β-galactosidase (Oxford Glycosystems) in 25 μl of 50 mM sodium acetate buffer, pH 3.5, containing 38 μg/ml BSA, for 16 h at 37 °C. All reactions were terminated by heating at 100 °C for 5 min. The products were desalted by passage through a column of 0.2 ml of AG50X12 (H^+), over 0.2 ml of AG3X4 (OH^-) over 0.1 ml of QAE-Sephadex A-25. Eluates were dried, and the residual acetic acid was removed by co-evaporation with 50 μl of toluene (two times).

Compositional Analysis and Methylation Analysis—Amino acids, ethanolamine, 2-aminoethylphosphonate, and glucosamine were quantified after strong acid hydrolysis (6 M HCl, 110 °C, 16 h) and derivatization with phenylisothiocyanate using a Waters Pico-Tag system, as described (22). Gas chromatography-mass spectrometry (GC-MS) analyses were performed with a Hewlett-Packard 5890-5970 system. The *myo*-inositol content of samples was measured using selected ion monitoring after strong acid hydrolysis and trimethylsilyl derivatization (22). Monosaccharide and lipid contents were measured after methanolysis, re-*N*-acetylation, and trimethylsilyl derivatization (22). Methylation linkage analysis was performed as described (22).

Electrospray-Mass Spectrometry—ES-MS data were obtained with a VG-Quattro triple-quadrupole mass spectrometer (Fisons Instruments, United Kingdom) coupled to a Michrom microbore HPLC system. Analysis of PI fractions was performed in negative ion mode, and aliquots of PI samples (20 μl of PI dissolved in chloroform/methanol/water (10:10:3, by volume)) were injected into the electrospray source at 5 μl/min. Source and spectrometer parameters were optimized using a standard of soybean PI (26). The masses of the released *O*-linked oligosaccharitol components were determined in negative ion mode. Samples, dissolved in 20 μl of 50% acetonitrile, were injected into the electrospray source at 5 μl/min. Source and spectrometer conditions were optimized using a standard of maltoheptaose (Sigma).

^{1}H NMR—One-dimensional 500-MHz ^{1}H NMR spectra of the individual oligosaccharitols were obtained using a Bruker AM 500 spectrometer equipped with a 5-mm triple resonance probe, and the samples were dissolved in 0.5 ml of ^2H_2O after repeated exchange in ^2H_2O. All experiments were performed at 300 K, and chemical shifts were referenced externally to acetone (2.225 ppm). Further assignments for oligosaccharitol *c* were deduced from two-dimensional ^{1}H-^{1}H experiments. Correlated spectroscopy and triple quantum-filtered correlated spectroscopy experiments were performed using a sweep width of 2,200 Hz, and 4,000 data points, and 512 increments were collected in f1. The rotating frame Overhauser effect spectroscopy experiment used 64 transients of 4,000 data points, and 1,024 increments were collected in f1. The spectral width collected was 4,400 Hz in each domain, and the mixing time was 500 ms. In the total correlation spectroscopy experiment, 64 transients of 4,000 datapoints were collected, and 512 experimental increments were collected in f1. The sweep width was 1,500 Hz, and the mixing time used was 203 ms.

Trans-sialylation of Mucin O-Linked Oligosaccharitols—Purified radiolabeled neutral oligosaccharitols, obtained after fractionation on the Glycoplex™ HPLC column, were dried in a speed-vac and redissolved in 0.02 M HEPES buffer (pH 7.0), 1 mM 3′-sialyllactose (SAα2–3Galβ1–4Glc) (Boehringer Mannheim), 0.2% bovine serum albumin (Ultrapure, Boehringer Mannheim) and incubated with purified *T. cruzi* TS (27). After 2 h at 37 °C, the reaction was stopped by the addition of 1 ml of water, and the amount of nonsialylated products was quantified by passage through a 0.5-ml QAE-Sephadex A-25 column equilibrated in water. Sialylated products were recovered after washing the column with 8 ml of water and elution with 1 ml of 1 M ammonium formate. Alternatively, the products were adjusted to 5 mM sodium acetate buffer, pH 4.0, and chromatographed on a Mono Q column, as described in Ref. 28, to determine the extent of sialylation of each individual oligosaccharide.

RESULTS

The mucins were purified from epimastigotes and metacyclic trypomastigotes by solvent extraction and octyl-Sepharose chromatography. The material recognized by the monoclonal antibody 10D8, specific for the sialic acid acceptors, eluted at 25% (v/v) propan-1-ol and appeared as two bands with apparent molecular masses of 35 and 50 kDa on SDS-polyacrylamide gel electrophoresis, as shown previously for the metacyclic trypomastigote sialic acid acceptors (12). The significance of the double nature of the antigen is unknown, but it may reflect the presence of at least two different (*O*-glycosylated/GPI-anchored) gene products. The purified mucins were judged to be free of *T. cruzi* LPPG, which migrates near the front of an SDS-polyacrylamide electrophoresis gel, by silver staining and by Western blot analysis using an LPPG-specific antibody (data not shown). Based on the *myo*-inositol content of the recovered material (25 nmol/10^{10} cells), the metacyclic mucin is present at a minimum of 1.5×10^6 copies/parasite. The mucins eluted from the octyl-Sepharose column were subjected to compositional analysis, showing that amino acids (particularly Ser and Thr) and monosaccharides (Man, Gal, GlcNAc, and SA) together with *myo*-inositol, ethanolamine, 1-*O*-hexadecylglycerol, and fatty acids were present in both preparations in amounts similar to those reported previously (8, 12). In addition, a previously unidentified peak in the amino acid analyses (with a retention time of 3.2 min) was shown to co-elute with an authentic standard of 2-aminoethylphosphonate (2-AEP). The molar ratio of ethanolamine to 2-AEP was approximately 1:1 for both preparations.

GPI Lipid Structure—The mucins (approximately 20 nmol of each, based on *myo*-inositol content) were subjected to nitrous acid deamination and extracted with butan-1-ol. The butan-1-ol extracts, containing the released PI moieties, were analyzed by ES-MS. The mucin isolated from epimastigotes produced one major pseudomolecular ion at *m/z* 795.5 and minor ions at *m/z* 809.6 and 823.6 (Fig. 1*A*). No other ions were observed in the mass range *m/z* 400-1400 (data not shown). The collision-induced dissociation daughter ion spectra of the *m/z* 823 and 795 parent ions (Fig. 1, *C* and *D*), define the parent ions as the $[M-1]^-$ pseudomolecular ions of 1-*O*-($C_{16:0}$)alkyl-2-*O*-($C_{18:0}$)acylglycerol-3-HPO_4-inositol and 1-*O*-($C_{16:0}$)alkyl-2-*O*-($C_{16:0}$)acylglycerol-3-HPO_4-inositol, respectively. The common daughter ions at *m/z* 79, 241, and 377 correspond to $[PO_3]^-$, [inositol-1,2-cyclic-phosphate]$^-$, and $[HPO_4\text{-}CH{=}CH\text{-}CH_2\text{-}O\text{-}(CH_2)_{15}\text{-}CH_3]^-$, respectively. The daughter ions at *m/z* 283 (*panel C*) and 255 (*panel D*) correspond to the carboxylate ions $[CH_3\text{-}(CH_2)_{16}\text{-}CO_2]^-$ and $[CH_3\text{-}(CH_2)_{14}\text{-}CO_2]^-$, respectively.

In contrast, the mucin from metacyclics showed, in addition to the same alkylacyl-PI pseudomolecular ion species at *m/z* 795.5 and 823.6, abundant ions at *m/z* 892.7 and 780.6 (Fig. 1*B*). The daughter ion spectra of these species (Fig. 1, *E* and *F*) define these ions as the $[M-1]^-$ pseudomolecular ions of inositol phosphoceramides (ceramide-PIs). In this case, the daughter ion spectra contain common ions at *m/z* 79, 97, 241, and 259, corresponding to $[PO_3]^-$, $[H_2PO_4]^-$, [inositol-1,2-cyclic-PO_4]$^-$, and [inositol-1-HPO_4]$^-$, respectively. The relatively stable amide bond of the ceramide prevents the formation of the carboxylate ions seen previously for the alkylacyl-PI species. The *m/z* values of the pseudomolecular ions at *m/z* 892.7 and 780.6 suggest that the ceramide components are made up of a sphinganine ($C_{18:0}$) long chain base and $C_{24:0}$ and $C_{16:0}$ fatty acids, respectively. The minor pseudomolecular ions at *m/z* 890.7 and

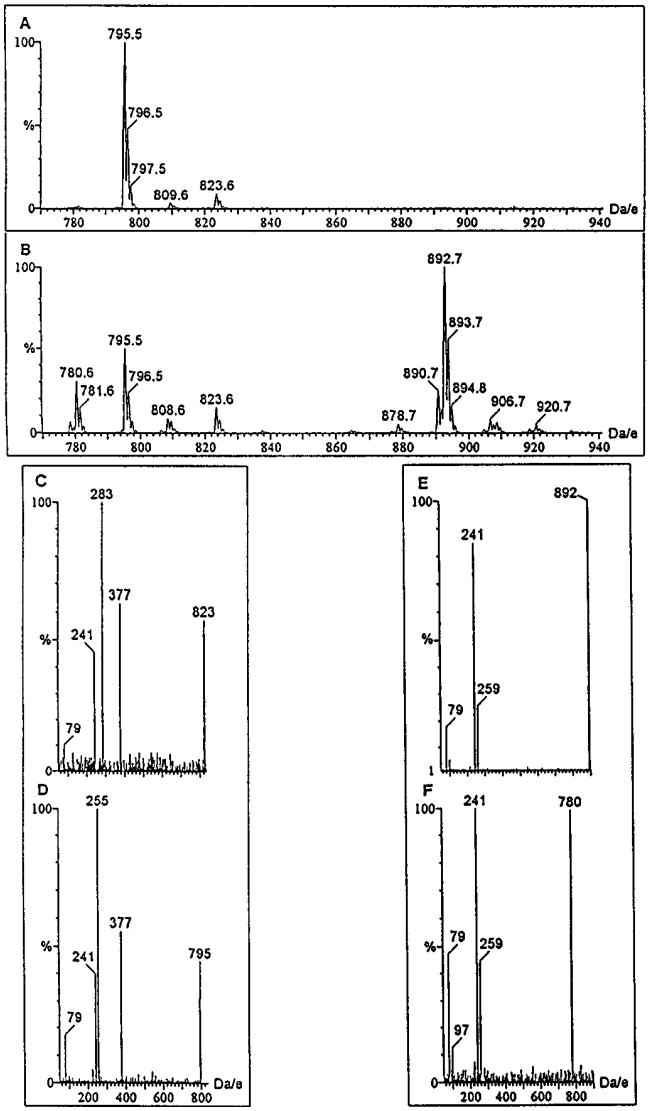

FIG. 1. **Negative ion electrospray mass spectra of the mucin PI moieties.** The PI moieties released from the epimastigote and metacyclic mucins (*panels A* and *B*, respectively) by nitrous acid deamination were recovered by solvent extraction and analyzed by ES-MS. The identities of major species detected in the epimastigote (*panel A*, *m/z* 823 and 795) and metacyclic (*panel B*, *m/z* 892 and 780) PI fractions were corroborated by the collision-induced dissociation daughter ion spectra (*panels C* and *D* and *panels E* and *F*, respectively).

778.6 most likely represent ceramide-PIs containing sphingosine ($C_{18:1}$) or mono-unsaturated fatty acids. The collision-induced daughter ion spectra of the *m/z* 795.5 and 823.6 ions were identical to those shown in *panels C* and *D* (data not shown). The relative proportions of all of different PI species and the tentative identification of some of the very minor species are given in Table I.

Structure of the GPI Glycan—To determine the structure of the GPI glycans, the aqueous phase obtained after butan-1-ol extraction of the deaminated mucins was reduced with NaB^3H_4 and dephosphorylated with aqueous HF, and the resulting GPI neutral glycans were purified by paper chromatography and high voltage paper electrophoresis. The neutral glycan fractions were chromatographed by Dionex HPAEC and Bio-Gel P4 gel filtration (data not shown). The neutral glycans derived from the epimastigotes and metacyclic trypomastigotes mucins eluted as one major component on both systems with chromatographic values of 3.0 Dionex units and 5.2 Gu, respectively. These values are identical to those of authentic Manα1–2Manα1–2Manα1–6Manα1–4AHM* (Man4-AHM*) (22). This sequence was confirmed by exoglycosidase digestion and partial acetolysis followed by product analysis by HPTLC (Fig. 2*A*). For the neutral glycans derived from both mucins, digestion with Manα1–2Man-specific *A. saitoi* α-mannosidase yielded a major product that comigrated with Manα1–6Manα1–4AHM* (Man2-AHM*) (Fig. 2*A*, *lanes 2* and *6*); partial acetolysis, which selectively hydrolyzes Manα1–6Man glycosidic bonds, produced a major product that comigrated with Manα1–4AHM* (Man1-AHM*) (Fig. 2*A*, *lanes 3* and *7*), and jack bean α-mannosidase, which removes all unsubstituted nonreducing terminal αMan residues, produced a major product that comigrated with AHM*. One additional minor neutral glycan structure, with a slower mobility than Man4-AHM*, was also detected in metacyclic and epimastigote preparations (Fig. 2*A*, *lanes 1* and *5*). This additional band can be seen more clearly in Fig. 2*B*, which shows the results for the epimastigote neutral glycan fraction before and after the sequencing digestions. This additional band was sensitive to *A. saitoi* α-mannosidase, producing a faint band migrating between Man2-AHM* and Man3-AHM* (Fig. 2*B*, *lane 2*), and digestion with jack bean α-mannosidase produced, in addition to the AHM*, a product that migrated slightly ahead of Man2-AHM* (Fig. 2*B*, *lane 4*). Thus, this minor component probably represents a Man4-AHM* structure with an additional, jack bean α-mannosidase-resistant residue linked to the first αMan adjacent to the AHM* (*i.e.* Manα1–2Manα1–2Manα1–6(*X*-)Manα1–4AHM*. Due to the low abundance of this glycan, its structure was not studied further.

Location of the Phosphoryl/Phosphonyl Substituents in the Glycan—Samples of the deaminated and NaB^3H_4-reduced epimastigote and metacyclic mucins were subjected to partial acid hydrolysis, using conditions that retain phosphoryl and phosphonyl substituents but partially cleave glycosidic bonds (23). The hydrolysates were then split into aliquots and (i) dephosphorylated with aqueous HF, (ii) treated with jack bean α-mannosidase prior to dephosphorylation with aqueous HF, or (iii) passed through a QAE-Sephadex A-25 ion exchange column. The products of these treatments were analyzed by HPTLC (Fig. 3). The dephosphorylated samples produced ladders of the components Man4-AHM*, Man3-AHM*, Man2-AHM*, Man1-AHM*, and AHM* (Fig. 3, *lanes 2* and *6*). In contrast, all of the bands except for Man3-AHM* and AHM* were diminished in the samples treated with mannosidase prior to dephosphorylation (Fig. 3, *lanes 3* and *7*). At least part of the less intense bands, migrating below Man3-AHM* and above Man2-AHM*, probably originated from the Manα1–2Manα1–2Manα1–6(*X*-)Manα1–4AHM*-containing mucin species. This result indicates that the Man3-AHM* component was fully protected from α-mannosidase digestion by an aqueous HF-sensitive substituent attached to the third αMan residue distal to the AHM*. This substituent is most likely an ethanolamine phosphate moiety, attached to the 6-position of the third αMan residue, that is the conventional GPI anchor bridge to the polypeptide chain (29). Another possibility is that part of this aqueous HF-sensitive substituent is 2-aminoethylphosphonate, as described for the GPI of epimastigote mucin of Y strain (17). Both ethanolamine and 2-aminoethylphosphonate were identified in the compositional analyses of the epimastigote and metacyclic trypomastigote mucins. When the partial acid hydrolysis products were passed through QAE-Sephadex, most of the Man4-AHM*, Man3-AHM*, Man2-AHM*, Man1-AHM*, and AHM* radioactivity was lost, indicating that all of the GPI glycans were negatively charged prior to dephosphorylation. This, in turn, suggests that most of the AHM* residues were originally substituted with phosphoryl (*i.e.* ethanolamine phosphate) and/or phosphonyl (*i.e.* 2-AEP) substituents, both of

TABLE I
Inositol-phospholipid composition of T. cruzi mucins

Lipid composition of 1-*O*-alkyl-2-*O*-acylglycerols		[M-1]$^-$ of the inositol-phospholipid	Relative abundance of each species[a]	
1-*O*-Alkylglycerol	2-*O*-Acyl fatty acid		*epi*-Mucin	*meta*-Mucin
		m/z	%	
1-*O*-Hexadecylglycerol	$C_{16:0}$	795.5	91	24
1-*O*-Hexadecylglycerol	$C_{18:0}$	823.6	9	7

Lipid composition of ceramides		[M-1]$^-$ of the inositol-phospholipid	Relative abundance of each species	
Long chain base	Amide-linked fatty acid		*epi*-Mucin	*meta*-Mucin
		m/z	%	
C_{18} sphinganine	$C_{16:0}$	780.6	0	15
C_{18} sphinganine	$C_{18:0}$	808.6	0	4
C_{18} sphinganine	$C_{24:0}$	892.7	0	48
C_{18} sphinganine	$C_{26:0}$	920.7	0	2

[a] Estimated from the relative abundances of the [M-1]$^-$ pseudomolecular ions.

which have been found attached to the 6-position of the GlcN residue of kinetoplastid GPI structures (29). The nature of the intense radioactive bands running below the Man4-AHM* band (Fig. 3, *lanes 4* and *8*) is unknown. However, these samples (unlike those in *lanes 2*, *3*, *6*, and *7*) had not undergone high voltage paper electrophoresis prior to analysis and may be non-carbohydrate radiochemical contaminants. The deduced structures of the GPI anchors for the epimastigote and metacyclic trypomastigote mucin are shown in Fig. 4.

Structure of the O-Linked Oligosaccharides of the Epimastigote and Metacyclic Trypomastigote Mucins—The *O*-linked oligosaccharides were released by β-elimination in the presence of NaB^2H_4 or NaB^3H_4, desialylated with neuraminidase, and separated on a Glycoplex™ hydrophilic interaction HPLC column. The column profiles revealed the presence of 6 major peaks (*peaks a–f*) that were similar in both preparations (Fig. 5, *A* and *B*). The purity of individual neutral oligosaccharides was assessed by HPTLC (Fig. 5*C*). The migration on HPTLC followed the separation in the Glycoplex™ column, except for oligosaccharide *b* (identified as Gal*f*β1–4GlcNAc-ol; see below), which was found to migrate slightly ahead of fraction *a* (GlcNAc-ol). The two minor fractions, labeled *b′* and *d′* were shown to contain unique structures that have not been fully characterized in this study. The structures of the components of *peaks a–f* are shown in Fig. 6. The experimental data supporting these assignments are given below.

Peak a contained a component that produced an [M-1]$^-$ pseudomolecular ion at *m/z* 223 in negative ion ES-MS and that contained only [1-^{2}H]GlcNAc-ol, as judged by GC-MS composition analysis (Table II). These data define *peak a* as the alditol GlcNAc-ol.

Peak b contained a component that produced an [M-1]$^-$ pseudomolecular ion at *m/z* 385 in negative ion ES-MS (deutero-reduced Hex-HexNAc-ol = 386 Da) and that contained only [1-^{2}H]GlcNAc-ol and Gal, as judged by GC-MS composition analysis (Table II). The GC-MS methylation analysis revealed the presence of a terminal Gal*f* residue and 4-*O*-substituted [1-^{2}H]GlcNAc-ol (Table II). The radiolabeled (NaB^3H_4-reduced) form of this component had a size of 3.5 Gu that was reduced to 2.6 Gu (the size of HexNAc-ol) after cleavage of the Gal*f* residue by mild acid hydrolysis (Table IV). The chemical shift (5.154 ppm; Table II) and extremely small $J_{1,2}$ coupling constant (data not shown), of the Gal*f* H-1 proton defined the galactofuranosidic linkage as β (8). Taken together, these data define the *peak b* component as Gal*f*β1–4GlcNAc-ol.

Peak c contained a component that produced an [M-1]$^-$ pseudomolecular ion at *m/z* 547 in negative ion ES-MS (deutero-reduced Hex_2-HexNAc-ol = 548 Da) and that contained only [1-^{2}H]GlcNAc-ol and Gal, as judged by GC-MS composition analysis (Table II). The GC-MS methylation analysis re-

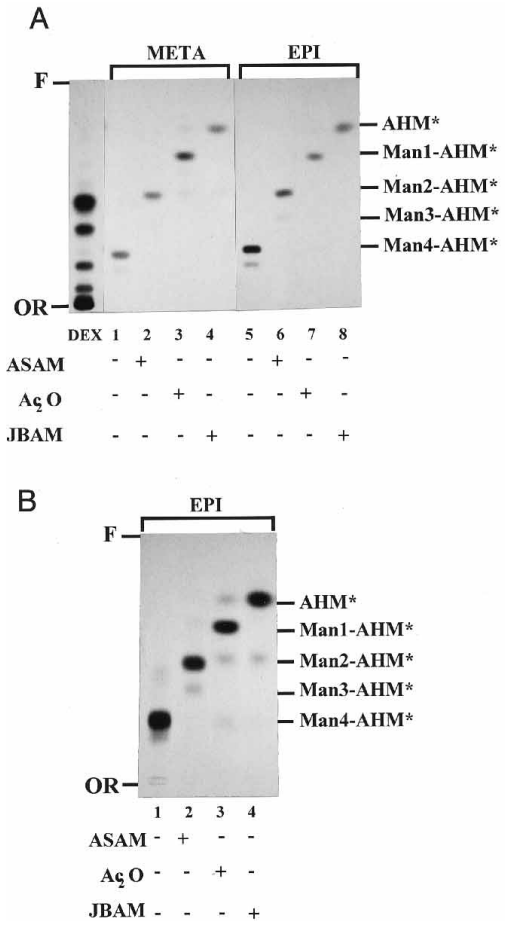

FIG. 2. **Sequential exoglycosidase digestion and partial acetolysis of GPI neutral glycans.** *A*, neutral glycans from epimastigotes (*EPI*) and metacyclic trypomastigote (*META*) mucins were obtained by nitrous acid deamination and reduction with NaB^3H_4, followed by aqueous HF treatment, and microsequenced by exoglycosidase digestion and partial acetolysis as described under "Materials and Methods." The labeled glycans were analyzed by HPTLC in solvent system A without treatment (*lanes 1* and *5*) or after *A. saitoi* α-mannosidase (*lanes 2* and *6*), partial acetolysis (Ac_2O)(*lanes 3* and *7*) or jack bean α-mannosidase (*lanes 4* and *8*) digestions. On the *right side* are indicated the migration positions of Manα1–2Manα1–2Manα1–6Manα1–4AHM (Man4-AHM*); Manα1–2Manα1–6Manα1–4AHM* (Man3-AHM*); Manα1–6Manα1–4AHM* (Man2-AHM*); Manα1–4AHM* (Man1-AHM*); and 2,5-anhydromannitol (AHM*) standards obtained from *T. cruzi* LPPG. DEX is ^{3}H-reduced dextran hydrolysate standard. *F* corresponds to the solvent front and *OR* to the origin. *Panel B* shows an additional HPTLC of epimastigote neutral glycan, with a longer exposure time.

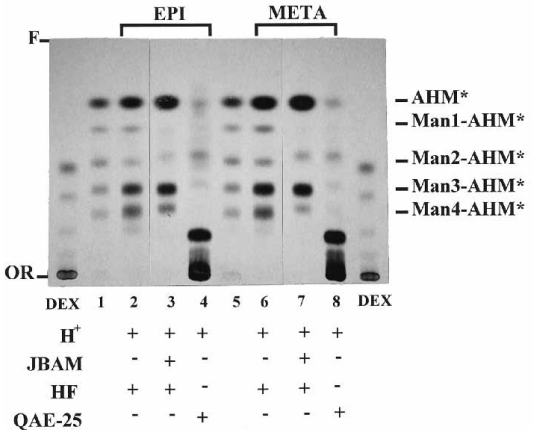

FIG. 3. **Location of phosphoryl/phosphonyl substituents.** HPTLC analysis of the mucins subjected to partial acid hydrolysis followed by sequential exoglycosidase digestion and dephosphorylation. Deaminated and reduced mucins from epimastigotes (*EPI*) and metacyclic trypomastigote (*META*) mucins were subjected to partial acid hydrolysis (H^+) followed by aqueous HF dephoshorylation (*HF*) (*lanes 2* and *6*), partial acid hydrolysis, jack bean α-mannosidase digestion, and aqueous HF dephosphorylation (*lanes 3* and *7*) or to partial acid hydrolysis and passage through QAE-Sephadex A-25 column (*lanes 4* and *8*). The products were analyzed by HPTLC in solvent A and fluorography. The migration of standards (*DEX*), and the glycans of *T. cruzi* LPPG (as described in Fig. 2) are shown in *lanes 1* and *5*.

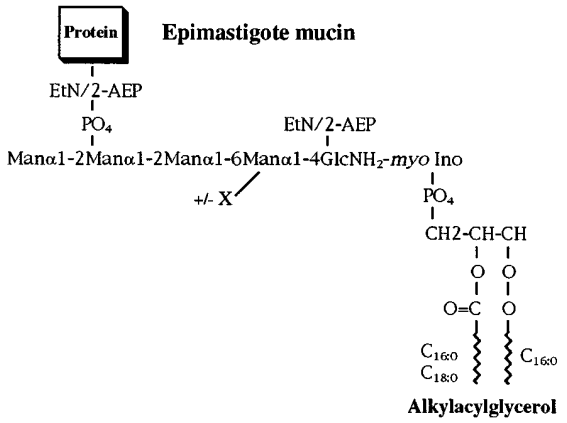

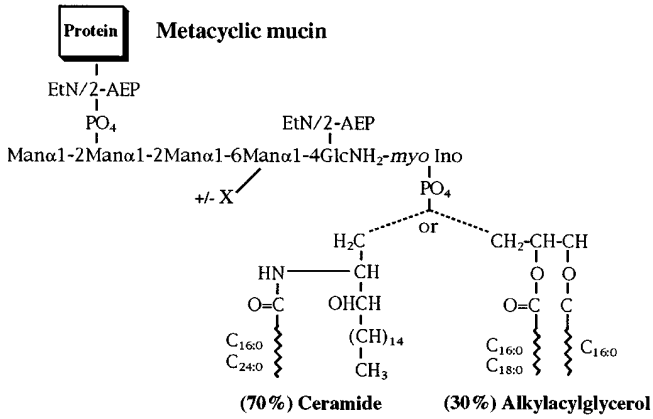

FIG. 4. **Proposed GPI anchor structures of *T. cruzi* mucins.** See text for details.

vealed the presence of a terminal Gal*f* residue, a terminal Gal*p* residue, and 4,6-di-*O*-substituted [1-^{2}H]GlcNAc-ol. The radiolabeled (NaB^{3}H$_4$-reduced) form of this component had a size of 4.5 Gu that was reduced to 3.5 Gu after cleavage of the Gal*f* residue by mild acid hydrolysis or after the cleavage of the βGal*p* residue with jack bean β-galactosidase (Table IV). The

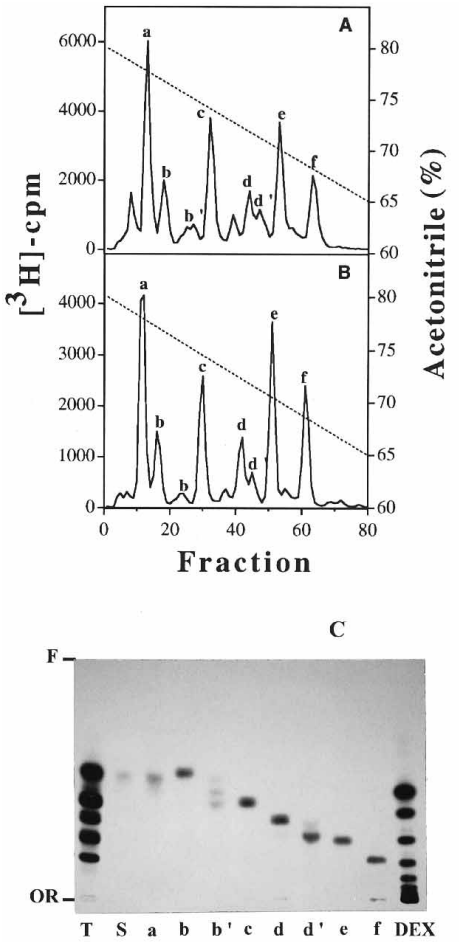

FIG. 5. **Fractionation of mucin oligosaccharitols released by reductive β-elimination.** Epimastigote (*panel A*) and metacyclic trypomastigote (*panel B*) mucins were submitted to mild alkaline β-elimination, with concomitant reduction with NaB^{3}H$_4$, and separated by HPLC using a Glycoplex™ column, as described under "Materials and Methods." *C*, the purity of individual oligosaccharitols from metacyclic sample (*lanes a–f*) *versus* the unfractionated oligosaccharitol mixture (*lane T*) was accessed by HPTLC in solvent system B. *Lane S* contains a [1-^{3}H]GlcNAc-ol standard, and *lane DEX* contains the ^{3}H-reduced dextran hydrolysate standard.

sensitivity of the structure to jack bean β-galactosidase, which does not efficiently cleave Gal*p*β1–4GlcNAc-ol, and its resistance to bovine testicular β-galactosidase, which does cleave Gal*p*β1–4GlcNAc-ol (16), suggest that the βGal*p* residue is attached to the 6-position of the GlcNAc-ol residue and that the *peak c* component has the structure Gal*p*β1–6(Gal*f*β1–4)GlcNAc-ol. The chemical shifts of the protons of this component (Table III), which are identical to those described in (8) for the same structure, confirm this assignment. The data in Table III add some additional assignments compared with Ref. 8: (i) the H-5 resonance of the βGal*p* residue, which was assigned by chemical shift arguments in Ref. 8, was confirmed from the rotating frame Overhauser effect spectroscopy experiment, and (ii) the H-6′ proton of the βGal*f* residue was assigned via the triple quantum-filtered correlated spectroscopy experiment, which is selective for the H-5, H-6, and H-6′ protons.

Peak d contained a component that produced an $[M-1]^-$ pseudomolecular ion at m/z 709 in negative-ion ES-MS (deutero-reduced Hex_3-HexNAc-ol = 710 Da) and that contained only [1-^{2}H]GlcNAc-ol and Gal, as judged by GC-MS composition analysis (Table II). The GC-MS methylation analysis revealed the presence of a terminal Gal*f* residue, a terminal Gal*p* residue, a 3-*O*-substituted Gal*p* residue, and 4,6-di-*O*-substi-

tuted [1-^{2}H]GlcNAc-ol. The radiolabeled (NaB^{3}H$_4$-reduced) form of this component had a size of 5.6 Gu that was reduced to 4.5 Gu after cleavage of the Gal*f* residue by mild acid hydrolysis and to 3.5 Gu after the cleavage of 2 βGal*p* residues with jack bean β-galactosidase (Table IV). Taking into account the methylation data, the accessibility of both βGal*p* residues to jack bean β-galactosidase suggests that they are linked together in the form Gal*p*β1–3Galβ1-. The bovine testicular β-galactosidase enzyme was capable of removing the terminal β1–3-linked Gal residue only, to yield a 4.5-Gu product, again suggesting that the βGal*p* branch was attached to the 6-position of the GlcNAc-ol residue. Taken together, these data suggest that the *peak d* component has the structure Gal*p*β1–3Gal*p*β1–6(Gal*f*β1–4)GlcNAc-ol. The chemical shifts of the anomeric protons of this component (Table II), which are identical to those described in Ref. 8 for the same structure, confirm this assignment.

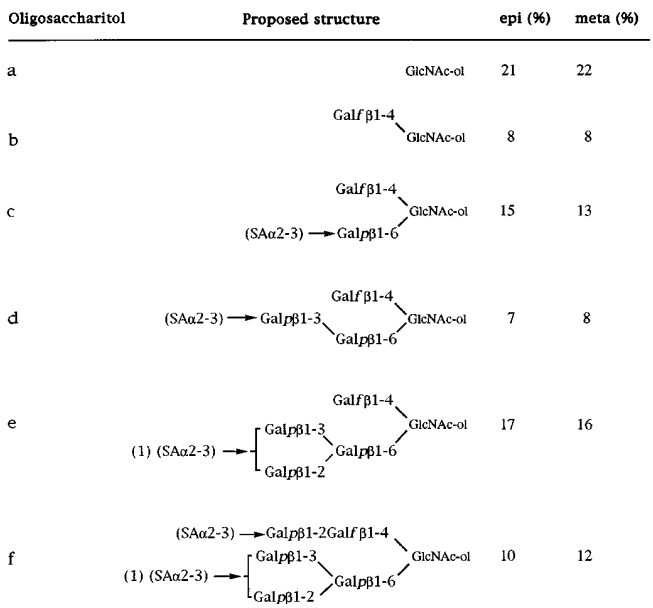

FIG. 6. **Proposed structures of the *O*-linked oligosaccharitols released from epimastigote and metacyclic trypomastigote mucins.** The structures were deduced as described in the text, except that the sialylation patterns are inferred from the SA transfer experiments described in Fig. *7*. The relative percentage of each structure was based on the recovery of each peak relative to the labeled material as shown in Fig. *5*.

Peak e contained a component that produced an [M-1]$^-$ pseudomolecular ion at *m/z* 871 in negative ion ES-MS (deutero-reduced Hex$_4$-HexNAc-ol = 872 Da) and which contained only [1-^{2}H]GlcNAc-ol and Gal, as judged by GC-MS composition analysis (Table II). The GC-MS methylation analysis revealed the presence of a terminal Gal*f* residue, two terminal Gal*p* residues, a 2,3-di-*O*-substituted Gal*p* residue, and 4,6-di-*O*-substituted [1-^{2}H]GlcNAc-ol. The radiolabeled (NaB^{3}H$_4$-reduced) form of this component had a size of 6.4 Gu that was reduced to 5.4 Gu after cleavage of the Gal*f* residue by mild acid hydrolysis (Table IV). Interestingly, the structure was resistant to both jack bean β-galactosidase and bovine testicular β-galactosidase enzymes.[2] The chemical shifts of the anomeric protons of this component (Table II) are identical to those described in Ref. 8 for the structure Gal*p*β1–3(Gal*p*β1–2)Gal*p*β1–6(Gal*f*β1–4)GlcNAc-ol, and all of the above data are consistent with this structure.

Peak f contained a component that produced an [M-1]$^-$ pseudomolecular ion at *m/z* 1,033 in negative ion ES-MS (deutero-reduced Hex$_4$-HexNAc-ol = 1,034 Da) and that contained only [1-^{2}H]GlcNAc-ol and Gal, as judged by GC-MS composition analysis (Table II). The radiolabeled (NaB^{3}H$_4$-reduced) form of this component had a size of 7.1 Gu that was reduced to 5.5 Gu after mild acid hydrolysis, suggesting that the structure contained either 2 Gal*f* residues or 1 Gal*f* residue that is substituted by a Gal*p* residue (Table IV). The structure was resistant to both jack bean β-galactosidase and bovine testicular β-galactosidase enzymes.[2] The chemical shifts of the anomeric protons of this component (Table II) are identical to those described in Ref. 8 for the structure Gal*p*β1–3(Gal*p*β1–2)Gal*p*β1–6(Gal*p*β1–2Gal*f*β1–4)GlcNAc-ol, and all of the above data are consistent with this structure.

trans-Sialidase Acceptor Activity of the O-Linked Oligosaccharides—Neuraminidase-treated, HPLC-purified, and radiolabeled oligosaccharitols were incubated with purified TS and 3′-sialyllactose as sialic acid donor, and the reaction products were fractionated by QAE-Sephadex chromatography. As expected, all of the oligosaccharitols containing terminal βGal*p*

[2] A number of useful details about the substrate specificities of jack bean β-galactosidase and bovine testes β-galactosidase can be deduced from this study: (i) neither enzyme can digest an oligosaccharide terminating in Gal*p*β1–3(Gal*p*β1–2)βGal*p*; (ii) neither enzyme can digest an oligosaccharide terminating in Gal*p*β1–2βGal*f*; and (iii) bovine testes β-galactosidase cannot digest Gal*p*β1–6GlcNAc-ol.

TABLE II
Summary of mass spectrometry and ^{1}H NMR spectroscopy analysis of O-linked carbohydrates of mucins from metacyclic trypomastigotes

Glycoplex[a] peak	ES-MS analysis[b]	^{1}H NMR chemical[c] shifts					Methylation analysis[d]					
		Gal*f*	Gal*p*(1)	Gal*p*(2)	Gal*p*(3)	Gal*p*(4)	4-GlucNAc-ol	4,6-GlucNAc-ol	*t*-Gal*f*	*t*-Gal*p*	3-Gal*p*	2,3-Gal*p*
	m/z			*ppm*								
a	223 (HexNAc-ol)											
b	385 (Hex-HexNAc-ol)	5.154					+	−	+	−	−	−
c	547 (Hex$_2$-HexNAc-ol)	5.215	4.432				−	+	+	+	−	−
d	709 (Hex$_3$-HexNAc-ol)	5.217	4.493	4.613			−	+	+	+	+	−
e	871 (Hex$_4$-HexNAc-ol)	5.273	4.582	4.662	4.862		−	+	+	++[e]	−	+
f	1033 (Hex$_5$-HexNAc-ol)	5.534	4.642	4.656	4.850	4.603			ND[f]			

[a] Components contained GlcNAc-ol (*a–f*) and Gal (*b–f*) by GC-MS compositional analysis.
[b] [M-1]$^-$ pseudomolecular ions detected by negative-ion ES-MS.
[c] Data obtained from one-dimensional 500-MHz NMR spectroscopy. Chemical shifts were referenced relative to acetone (2.225 ppm.) at 300 K.
[d] Obtained from analysis of partially methylated alditols acetate (PMAAs).
[e] Two terminal Gal*p* residues detected.
[f] Not determined.

TABLE III
^1H NMR chemical shifts of oligosaccharitol c

Proton	βGal*f*	βGal*p*	GlcNAc-ol
H-1	5.21	4.43	3.73
H-1′			3.66
H-2	4.14	3.56	4.17
H-3	4.08	3.66	3.93
H-4	4.09	3.92	3.82
H-5	3.82	3.71	4.03
H-6	3.63	3.76	4.14
H-6′	3.72	3.78	3.84
NAc			2.06

TABLE IV
Bio-Gel P4 analysis of neutral O-linked carbohydrates of mucins from metacylic trypomastigotes

Individual *O*-linked carbohydrates separated on HPLC, were chromatographed on a Bio-Gel P4 column, and the elution position relative to a series of dextran oligomers was expressed as glucose units (Gu). The oligosaccharides were further treated with bovine testicular β-galactosidase (BTBG), jack bean β-galactosidase (JBBG) and 40 mM trifluoroacetic acid (TFA).

Oligosaccharide	Size on P4	Treatment		
		BTBG	JBBG	TFA
a	2.6	NT[a]	NT	NT
b	3.5	—[c]	—	2.6
c	4.5	—	3.5	3.5
d	5.6	4.5	3.5	4.5
e	6.4	—	—	5.4
f	7.1	—	—	5.5[b]

[a] NT, not treated.
[b] TFA treatment produced products correspondent to 7.0 and 5.5 Gu.
[c] No modification after treatment.

were sialylated, while the oligosaccharitol *b*, which contains only a terminal βGal*f* residue, was not a sialic acid acceptor (not shown). To further evaluate the degree of sialylation of oligosaccharitols *c–f*, the TS reaction products were fractionated in a Mono-Q column. Oligosaccharitols c and d, which contain single βGal*p* termini, accepted only one sialic acid residue, as expected (Fig. 7, *A* and *B*). Oligosaccharitol *e*, which contains two terminal βGal*p* residues (attached to the 2- and 3-position of the same subterminal residue) accepted only one sialic acid residue (Fig. 7*C*). This result indicates that either only one of the terminal βGal*p* residues can be sialylated or sialylation of either residue precludes sialylation of the adjacent residue for steric reasons. Oligosaccharitol *f*, which, compared with oligosaccharitol *e*, has one additional βGal*p* attached to a different branch, was both monosialylated and bisialylated (Fig. 7*D*). These sialylation patterns are included in Fig. 6.

DISCUSSION

We have compared the structures of the *O*-linked oligosaccharides and the GPI anchors of the major mucin-like SA acceptors from metacyclic trypomastigote and epimastigote forms of *T. cruzi*. We found that when epimastigotes transform into metacyclic trypomastigotes the *O*-linked oligosaccharides and the GPI glycan core structures remain unchanged, whereas the lipid portion of the GPI anchor changes substantially from alkylacylglycerol-PI to mostly ceramide-PI. The ES-MS analyses showed that the epimastigote mucins contain alkylacyl-PI species, the principal component being 1-*O*-hexadecyl-2-*O*-hexadecanoyl-PI, whereas 70% of the metacyclic mucins contain inositol phosphoceramides (ceramide-PIs), with the principal ceramide components identified as lignoceroyl-sphinganine and palmitoyl-sphinganine. The remaining 30% of the metacyclic mucins contain the same alkylacyl-PI species as the epimastigote mucins. The lipids present in the epimastigote mucins of strain Y, identified as 40/45-kDa glycoconjugates, were also shown to contain 1-*O*-hexadecyl-2-*O*-palmitoylglycerol and 1-*O*-hexadecyl-2-*O*-stearoylglycerol (17), in similar proportions to those found in G-strain epimastigotes in this study. The lipid portion of a molecule called lipophosphoglycan-like glycoconjugate, isolated from *T. cruzi* epimastigotes (Peru strain) also contains the same alkylacylglycerol-PI species (9). No direct evidence for the presence of phosphosaccharide repeats, characteristic of *Leishmania* lipophosphoglycans, was presented in that study, and, given its similarity in composition and properties to the mucin-like molecules reported here and in Refs. 8, 12, 16, and 17, it should be considered as a member of the *T. cruzi* mucin family.

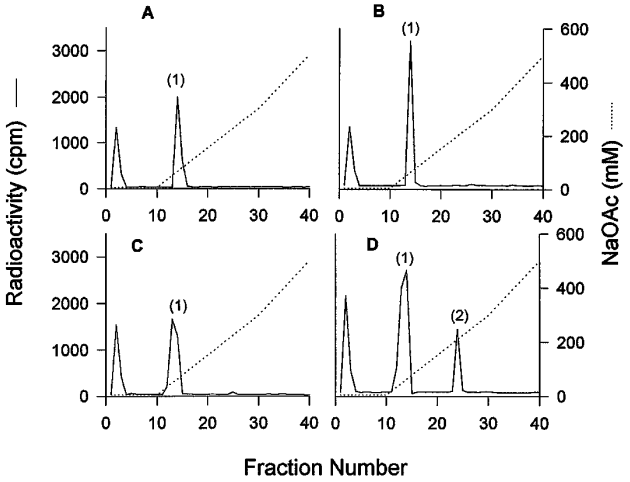

FIG. 7. **Sialylation of *O*-linked oligosaccharitols of metacyclic trypomastigote mucin accessed by Mono Q chromatography.** Purified and labeled neutral oligosaccharitols *c–f* (*panels A*, *B*, *C*, and *D*) of metacyclic trypomastigotes were incubated with TS and sialyllactose, as described under "Materials and Methods." After 3 h of incubation, the samples were diluted with 5 mM sodium acetate, pH 4.0, and loaded onto a Mono Q column. The *number above* each *peak* represents the amount of sialic acid residues per oligosaccharitol.

The GPI anchors of both trypomastigote Tc-85 (30) and the metacyclic 90-kDa 1G7-antigen (26, 31) have been shown to contain mostly 1-*O*-hexadecyl-2-acyl-PIs, which are similar to those reported here and in Refs. 9 and 17 for the epimastigote mucin GPI membrane anchors. In the case of the metacyclic mucins, the GPI anchor ceramide-PI structures are identical to the main types found in LPPG, the major surface glycoconjugate of *T. cruzi* (Y strain) epimastigotes (32, 33); *i.e.* they contain palmitoyl-sphinganine and lignoceroyl-sphinganine. The LPPG molecule also shares the same Man_4-GlcN core glycan structure as the mucin GPI anchor and contains a 2-AEP group attached to the 6-position of the GlcN residue (24, 32, 33). Thus, it is possible that these ceramide-PI anchors are biosynthetically related to LPPG. The putative point of biosynthetic divergence would be in the addition of the ethanolamine phosphate (or 2-AEP) bridge to Man_4-(2-AEP)GlcN-(ceramide-PI) to form the GPI anchor precursor or the addition of two terminal Gal*f* residues to form LPPG. The relationship between the ceramide-PI type GPI structures and the alkylacyl-PI structures is not clear. In the case of *Saccharomyces cerevisiae*, the GPI precursors are based on diacyl-PIs that on most (but not all) glycoproteins are exchanged to ceramide-PIs after transfer to protein in an as yet undefined lipid-remodelling reaction (34, 35). It is possible that a similar mechanism may operate in *T. cruzi*, as discussed in Ref. 26. The observation that all of the early GPI intermediates in *T. cruzi* epimastigotes are based on alkylacyl-PI is consistent with this notion (36). Interestingly, a glycoinositolphospholipid (called GIPL A) with the same glycan core structure as LPPG, but containing a lipid

moiety composed exclusively of 1-*O*-hexadecyl-2-*O*-palmitoyl-glycerol, has been detected in early cultures of Y strain *T. cruzi* epimastigotes (37). This glycoinositolphospholipid could be the immediate precursor to LPPG. If so, the shift from alkylacyl-PI to ceramide-PI seen in the mucins upon transformation of late epimastigotes to metacyclic trypomastigotes may be similar to the shift from GIPL A to LPPG seen upon the transformation from early to late epimastigotes. Thus the change in the PI lipid structure of the mucin molecules of *T. cruzi* appears to be under developmental control. Interestingly, the ES-MS analysis of the metacyclic 1G7-antigen PI moieties also revealed that a small quantity (>15 mol %) of the GPI anchors contained ceramide-PIs (26). However, in this case the ceramides were predominantly palmitoyl-sphinganine and stearoyl-sphinganine, and the reason for the lack of lignoceroyl-sphinganine is not clear. As Grace's medium was used to induce metacyclogenesis in the 1G7-antigen work, whereas liver infusion tryptose medium was used throughout this mucin study, it is possible that the nutrient conditions might affect the fatty acid content of the ceramide components.

The possibility that the ceramide-PI content of the metacyclic trypomastigote mucin preparation might be due to contamination with LPPG can be ruled out for the following reasons: (i) the mucin fractions were eluted from the octyl-Sepharose column between 23 and 27% propan-1-ol, while LPPG is known to elute from this column at >40% propan-1-ol (33); (ii) metacyclic trypomastigotes express about 10 times less LPPG than epimastigotes (38), suggesting that any LPPG contamination would be greater in epimastigote preparations; (iii) no LPPG could be detected in the mucin preparations by SDS-polyacrylamide gel electrophoresis and silver staining and by Western blot with an anti-LPPG antibody; (iv) the mucin samples were exhaustively pre-extracted with butan-1-ol to remove glycolipid and phospholipid contaminants prior to deamination; (v) the Man_3-AHM* fragment, generated by partial acid hydrolysis of the deaminated NaB^3H_4-reduced mucin, was completely protected from jack bean α-mannosidase digestion by an aqueous HF-sensitive substituent (Fig. 3, *lane 7*). The corresponding LPPG Man_3-AHM* fragment would be digested to AHM*.

The structure of the major GPI glycan (shown to be as Manα1–2Manα1–2Manα1–6Manα1–4GlcN-*myo*-inositol) was identical in epimastigote and metacyclic mucins. A small proportion of the GPI glycans contained an additional unidentified sugar residue attached to the αMan residue adjacent to the GlcN residue. Similar results have been reported recently for the epimastigote mucin of Y strain (17). The major Man_4 GPI glycan structure described above is also found in the 1G7-antigen (26), and this structure represents only a minor substitution of the conserved Man_3 GPI glycan found in all GPI anchors characterized to date (29). Interestingly, the GPI glycan core of one surface glycoprotein of infective trypomastigotes derived from mammalian cells contained a glycan core composed a Man_3-GlcN rather than a Man_4-GlcN (30).

The mucins from epimastigotes and metacyclic trypomastigotes also share the same *O*-linked oligosaccharide chains, linked to the protein backbone via *N*-acetylglucosamine residues rather than *N*-acetylgalactosamine that is commonly found in vertebrate mucins. In the case of *T. cruzi* mucins described here about 20% of the oligosaccharitols released by reductive β-elimination corresponded to non-substituted GlcNAc-ol. Most of the *O*-linked GlcNAc residues are substituted and might not be accessible. These substitutions included chains formed by one to five additional galactose residues, always with one βGal*f* residue linked to the 4-position of the GlcNAc. The remaining βGal*p* residues are mostly linked as linear and branched side-chains to the 6-position of the GlcNAc. The *O*-linked oligosaccharide structures determined in this study are identical to those found in the epimastigote mucin of G strain (8), except that the Gal*f*β1–4GlcNAc-ol structure was not described by these authors. Since Gal*p*β1–6GlcNAc-ol was not observed in this or any other study, we suggest that during biosynthesis the addition of the βGal*f* residue precedes the addition of the βGal*p* residues.

Studies of TS specificity have shown that the enzyme is able to sialylate unbranched terminal βGal*p* residues, and that substitutions near the Gal decrease the extent of sialylation (39, 40). We have confirmed these findings by using the purified *O*-linked oligosaccharides that are the natural acceptors on the parasite surface. The branched oligosaccharide *e*, that has two terminal βGal*p* residues, can accept only one SA, while the oligosaccharide *f*, that has one additional terminal βGal*p* residue, can accept a second SA. In agreement with these data, a maximum of two SA are incorporated per oligosaccharide *in vivo* (data not shown). The reasons why the branched oligosaccharide structure cannot accept two SA residues is unknown, but it is likely to be due to steric effects since the two terminal βGal*p* residues are attached to adjacent oxygen atoms on the penultimate Gal residue.

In summary, the major difference between epimastigote and metacyclic mucins is the acquisition of a high content of ceramide-PI in the metacyclic forms, in the place of alkylacyl-PI. Epimastigotes express large amounts of LPPG, which contains the same ceramide-PI species, indicating that acquisition of ceramide-PI in the mucin is not unique to metacyclic forms. The reason why the metacyclic mucins are anchored to the cell surface by a ceramide-PI, rather than an alkylacyl-PI, is unknown. However, it may be significant that the majority of the metacyclic mucins are shed by the parasite during host cell invasion, whereas the majority of the alkylacyl-PI anchored 1G7-antigen is retained on the parasite surface (12). Thus, surface-stability during invasion may be modulated by lipid remodelling of specific molecules. The structural changes in the mucin molecules upon metacyclogenesis are clearly less profound than those observed in the LPGs of the *Leishmania*, where the lipids remain unchanged but the type and/or number of phosphosaccharide repeats change dramatically (41, 42). Nevertheless, the mucin shedding phenomenon may make the subtle change in lipid structure equally important for the infectivity of *T. cruzi*.

Acknowledgments—We thank I. de Almeida, L. R. Travassos, and P. Schneider for helpful suggestions and discussions and J. O. Previato and L. Mendoça-Previato for making data available to us prior to publication. We also thank D. Neville for generous assistance with the GlycoMap.

REFERENCES

1. Colli, W. (1993) *FASEB J.* **7,** 1257–1264
2. Cross, G. A. M., and Takle, G. B. (1993) *Annu. Rev. Microbiol.* **46,** 385–411
3. Briones, M. R. S., Egima, C. M., Acosta, A., and Schenkman, S. (1994) *Exp. Parasitol.* **79,** 211–214
4. Schenkman, S., Eichinger, D., Pereira, M. E. A., and Nussenzweig, V. (1994) *Annu. Rev. Microbiol.* **48,** 499–523
5. Alves, M. J. M., and Colli, W. (1975) *FEBS Lett.* **52,** 188–190
6. Ferguson, M. A. J., Snary, D., and Allen, A. K. (1985) *Biochim. Biophys. Acta* **842,** 39–44
7. Previato, J. O., Andrade, A. F., Pessolani, M. C., and Mendoça-Previato, L. (1985) *Mol. Biochem. Parasitol.* **16,** 85–96
8. Previato, J. O., Jones, C., Gonçalves, L. P. B., Wait, R., Travassos, L. R., and Mendoça-Previato, L. (1994) *Biochem. J.* **301,** 151–159
9. Singh, B. N., Lucas, J. J., Beach, D. H., and Costello, C. E. (1994) *J. Biol. Chem.* **269,** 21972–21982
10. Yoshida, N., Mortara, R. A., Araguth, M. F., Gonzalez, J. C., and Russo, M. (1989) *Infect. Immun.* **57,** 1663–1667
11. Mortara, R. A., da Silva, S., Araguth, M. F., Blanco, S. A., and Yoshida, N. (1992) *Infect. Immun.* **60,** 4673–4678
12. Schenkman, S., Ferguson, M. A. J., Heise, N., Cardoso de Almeida, M. L., Mortara, R. A., and Yoshida, N. (1993) *Mol. Biochem. Parasitol.* **59,** 293–304
13. Andrews, N. W., Hong, K., Robbins, E. S., and Nussenzweig, V. (1987) *Exp. Parasitol.* **64,** 474–484
14. Schenkman, S., Jiang, M.-S., Hart, G. W., and Nussenzweig, V. (1991) *Cell* **65,**

1117–1125
15. Acosta, A., Schenkman, R. P. F., and Schenkman, S. (1994) *Braz. J. Med. Biol. Res.* **27,** 439–442
16. Almeida, I. C., Ferguson, M. A. J., Schenkman, S., and Travassos, L. R. (1994) *Biochem. J.* **304,** 793–802
17. Previato, J. O., Jones, C., Xavier, M. T., Wait, R., Travassos, L. R., Parodi, A. J., and Mendonça-Previato, L. (1995) *J. Biol. Chem.* **270,** 7241–7250
18. Ruiz, R. C., Rigoni, V. L., Gonzalez, J., and Yoshida, N. (1993) *Parasite Immunol.* **15,** 121–125
19. Yoshida, N. (1983) *Infect. Immun.* **40,** 836–839
20. Camargo, E. P. (1964) *Rev. Inst. Med. Trop. Sao Paulo* **6,** 93–100
21. McConville, M. J., and Blackwell, J. M. (1991) *J. Biol. Chem.* **266,** 15170–15179
22. Ferguson, M. A. J. (1993) in *Glycobiology: A Practical Approach* (Fukuda, M., and Kobata, A., eds) pp. 349–383, IRL Press, Oxford
23. Schneider, P., and Ferguson, M. A. J. (1995) *Methods Enzymol.* **250,** 614–630
24. de Lederkremer, R. M., Lima, C., Ramírez, M. I., Ferguson, M. A. J., Homans, S. W., and Thomas-Oates, J. (1991) *J. Biol. Chem.* **266,** 23670–23675
25. Turco, S. J., Orlandi, P. A., Jr., Homans, S. W., Ferguson, M. A. J., Dwek, R. A., and Rademacher, T. W. (1989) *J. Biol. Chem.* **264,** 6711–6715
26. Heise, N., Cardoso de Almeida, M. L., and Ferguson, M. A. J. (1995) *Mol. Biochem. Parasitol.* **70,** 71–84
27. Schenkman, S., Chaves, L. B., Pontes de Carvalho, L., and Eichinger, D. (1994) *J. Biol. Chem.* **269,** 7970–7975
28. Kobata, A., and Endo, T. (1993) in *Glycobiology: A Practical Approach* (Fukuda, M., and Kobata, A., eds) pp. 79–102, IRL Press, Oxford
29. McConville, M. J., and Ferguson, M. A. J. (1993) *Biochem. J.* **294,** 305–324
30. Couto, A. S., De Lederkremer, R. M., Colli, W., and Alves, M. J. M. (1993) *Eur. J. Biochem.* **217,** 597–602
31. Güther, M. L. S., Cardoso de Almeida, M. L., Yoshida, N., and Ferguson, M. A. J. (1992) *J. Biol. Chem.* **267,** 6820–6828
32. Previato, J. O., Gorin, P. A., Mazurek, M., Xavier, M. T., Fournet, B., Wieruszesk, J. M., and Mendonça-Previato, L. (1990) *J. Biol. Chem.* **265,** 2518–2526
33. Lederkremer, R. M., Lima, C., Ramírez, M. I., and Casal, O. L. (1990) *Eur. J. Biochem.* **192,** 337–345
34. Conzelmann, A., Puoti, A., Lester, R. L., and Desponds, C. (1992) *EMBO J.* **11,** 457–466
35. Sipos, G., Puoti, A., and Conzelmann, A. (1994) *EMBO J.* **13,** 2789–2796
36. Heise, N., Raper, J., Buxbaum, L. U., and Cardoso de Almeida, M. L. (1994) *Mem. Inst. Oswaldo Cruz* **89,** 98
37. Lederkremer, R. M., Lima, C. E., Ramírez, M. I., Gonçalves, M. F., and Colli, W. (1993) *Eur. J. Biochem.* **218,** 929–936
38. Golgher, D. B., Colli, W., Souto-Padrón, T., and Zingales, B. (1993) *Mol. Biochem. Parasitol.* **60,** 249–264
39. Vandekerckhove, F., Schenkman, S., Pontes de Carvalho, L., Tomlinson, S., Kiso, M., Yoshida, M., Hasegawa, A., and Nussenzweig, V. (1992) *Glycobiology* **2,** 541–548
40. Ferrero-García, M. A., Trombetta, S. E., Sánchez, D. O., Reglero, A., Frasch, A. C. C., and Parodi, A. J. (1993) *Eur. J. Biochem.* **213,** 765–771
41. McConville, M. J., Turco, S. J., Ferguson, M. A. J., and Sacks, D. L. (1992) *EMBO J.* **11,** 3593–3600
42. Sacks, D. L., Pimenta, P. F. P., McConville, M. J., Schneider, P., and Turco, S. J. (1995) *J. Exp. Med.* **181,** 685–697